FULL PAPER

Transparent InP Quantum Dot Light-Emitting Diodes with ZrO_2 Electron Transport Layer and Indium Zinc Oxide Top Electrode

Hee Yeon Kim, Yu Jin Park, Jiwan Kim, Chul Jong Han, Jeongno Lee, Yohan Kim, Tonino Greco, Christian Ippen, Armin Wedel, Byeong-Kwon Ju, and Min Suk Oh**

Because of outstanding optical properties and non-vacuum solution processability of colloidal quantum dot (QD) semiconductors, many researchers have developed various light emitting diodes (LEDs) using QD materials. Until now, the Cd-based QD-LEDs have shown excellent properties, but the eco-friendly QD semiconductors have attracted many attentions due to the environmental regulation. And, since there are many issues about the reliability of conventional QD-LEDs with organic charge transport layers, a stable charge transport layer in various conditions must be developed for this reason. This study proposes the organic/inorganic hybrid QD-LEDs with Cd-free InP QDs as light emitting layer and inorganic ZrO_2 nanoparticles as electron transport layer. The QD-LED with bottom emission structure shows the luminescence of 530 cd m^{-2} and the current efficiency of 1 cd/A. To realize the transparent QD-LED display, the two-step sputtering process of indium zinc oxide (IZO) top electrode is applied to the devices and this study could fabricate the transparent QD-LED device with the transmittance of more than 74% for whole device array. And when the IZO top electrode with high work-function is applied to top transparent anode, the device could maintain the current efficiency within the driving voltage range without well-known roll-off phenomenon in QD-LED devices.

1. Introduction

Next generation display technologies using colloidal quantum dot (QD) materials have attracted many attentions due to narrow full width at half maximum (FWHM), color tunability and solution processability.[1–6] These colloidal QD materials can be used as color converting materials for backlight unit in liquid crystal display (LCD) or light emitting materials for electroluminescence (EL) devices.[1–8] In the case of organic light emitting diode (OLED), we can find mobile display devices and large area OLED TVs in the commercial market now. But, since organic materials in the OLED can be degraded by oxygen or humidity in the air, an additional encapsulation technology have been very important.[9,10] If those organic materials in OLEDs are changed into inorganic materials, we can improve the reliability of devices for the long-term operation. Therefore, there have been many attempts to use inorganic colloidal QD semiconductors as light emission layer. Although there have been several good results about QD-LED devices, the most outstanding performances have been reported from the devices using Cd-based QD materials.[4–6] But, due to the restriction of hazardous substances (RoHS) compliance for QD display components, we need to use Cd-free QDs for display applications in the near future.[11] There are several candidates for eco-friendly colloidal QD materials such as indium phosphide (InP) and $CuInS_2$ (CIS).[12–16] But, since CIS QDs show larger FWHM than those of Cd-based and InP QD materials, they are not suitable for the EL applications.[15] And, in the case of charge transport layers, conventional QD-LED devices use organic charge transport layers. Due to the same reason as OLED devices, there must be degradation problems caused by oxygen or humidity. Therefore several research groups reported QD-LED devices with inorganic oxide charge transport layers and showed very improved performances recently.[3–6,12,16] Especially, the devices using CdSe QDs as emitting layer and ZnO nanoparticles as electron transport layer (ETL) showed excellent luminescence characteristics.[3,4] But, due to the large electron

H. Y. Kim, Y. J. Park, Dr. C. J. Han, Dr. J. Lee, Dr. M. S. Oh
Display Materials and Components Research Center
Korea Electronics Technology Institute (KETI)
Seongnam-si, Gyeonggi-do 463-816, Republic of Korea
E-mail: ohms@keti.re.kr
H. Y. Kim, Prof. B.-K. Ju
Display and Nanosystem Laboratory
College of Engineering
Korea University
Seoul 136-713, Republic of Korea
E-mail: bkju@korea.ac.kr
Prof. J. Kim
Department of Advanced Materials Engineering
Kyonggi University
Suwon-si, Gyeonggi-do 16227, Republic of Korea
Y. Kim, Dr. T. Greco, Dr. C. Ippen, Dr. A. Wedel
Fraunhofer Institute for Applied Polymer Research
Potsdam-Golm 14476, Germany

DOI: 10.1002/adfm.201505549

injection barrier between the ZnO ETL and the InP QDs, more suitable ETL should be applied to our devices. Among several candidates, such as SnO_2, TiO_2, zinc tin oxide (ZTO), ZnO, and ZrO_2, we choose ZrO_2 due to the similar conduction band (E_c) level to that of InP QDs.[5,17–19] Although the conventional ZrO_2 has been used as insulating layer, there was a report about OLED devices using ZrO_2 layer as electron injection layer (EIL) and they showed the improved performance because of better hole blocking ability of ZrO_2 associated with its deep valence band (E_v).[19] For this reason, we select ZrO_2 layer as ETL for InP QD-LED device application and show the feasibility of ZrO_2 layer for eco-friendly QD-LED.

And, recently, there have been many interests in the transparent display for various applications such as wearable, vehicle, and future displays. Until now, top emission and semi-transparent OLED or QD-LED display devices have used very thin metal layers for top transparent electrode.[20,21] But, to realize true transparent display, the transparent conductive oxide (TCO) which can show the high transparency and high conductivity, such as indium tin oxide (ITO) or indium zinc oxide (IZO), must be applied. But, the conventional process for the TCO electrode is sputtering deposition process. In this case, due to the sputtering damage on the organic layers under top electrode during deposition process, it has not been easy to realize fully transparent display in conventional OLED or QD-LED structure. To solve this kind of problem, there were several researches about fully transparent organic thin film transistor device with thin oxide layer between TCO source/drain electrodes and organic semiconductors by thermal evaporation and transparent oxide electrode by sputtering process on the thin oxide interlayer.[22,23]

In this report, to realize the transparent eco-friendly QD-LED devices, we fabricated the inverted QD-LED devices with Cd-free InP QDs as light emitting layer and ZrO_2 nanoparticles as electron transport layer by solution process. And, by using new deposition process for transparent electrode on organic semiconductors, we could realize the fully transparent (T_{panel} > 74% @ 550 nm) QD-LED display devices successfully by using new deposition process for transparent electrode on organic semiconductors.

2. Results and Discussion

2.1. Synthesis of Eco-Friendly QD and Basic Device Application

To fabricate eco-friendly QD-LEDs, we synthesized Cd-free QDs with InP semiconductor by simple heating-up method.[24,25] **Figure 1**a shows the simple schematic cross section and transmission electron microscopy (TEM) image of our InP QD core with ZnSe/ZnS double shell structure. The diameter of InP core is estimated to be ≈4.25 nm from the first exciton peak at 490 nm in absorbance data (Figure S1, Supporting Information). After ZnSe first shell of one monolayer and ZnS second shell of two monolayers were coated on InP core, the final particle size should be less than 6.1 nm theoretically. To confirm the size of QDs, we measured TEM images. As we can see in Figure 1a, the diameter of our InP QDs is about 5.5 nm which

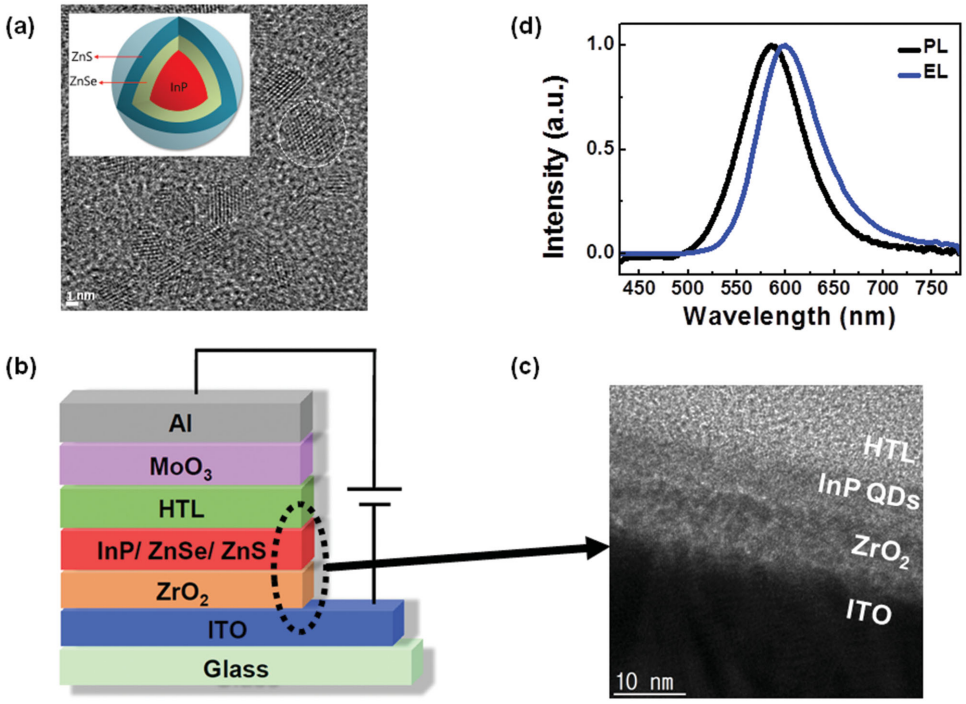

Figure 1. a) Schematic cross section and TEM image of InP/ZnSe/ZnS multi-shell QD. b) Basic device structure of InP QD-LED with Al top electrode. c) TEM image of HTL, InP QD, ZrO_2, and ITO. The thicknesses of InP QD, and ZrO_2 layers are about 5.9 and 8.9 nm respectively. d) PL and EL intensities versus wavelength of InP/ZnSe/ZnS QDs. The peak wavelengths of PL and EL data are 586 and 600 nm respectively. The peak wavelength shift from same QD semiconductor is 14 nm. FWHM values are 74 nm for PL and EL measurement.

is slightly smaller than the estimated value. Figure 1b displays the inverted structure of InP QD-LED unit device with inorganic ZrO_2 ETL. The ZrO_2 nanoparticles of about 3 nm diameter were spin coated on the patterned ITO cathode. Because the solvent for ZrO_2 nanoparticles can damage the QD layer, we chose the inverted structure different from other conventional QD-LED structures. Since the n-type oxide thin film transistors (TFTs) have been used for the pixel driving circuits in display panel recently, this inverted structure also can be helpful to the design of display pixel array. To improve the charge transport property, the ZrO_2 ETL was annealed by rapid thermal annealing (RTA) at 300 °C in vacuum.[26] After the annealing process of ZrO_2 ETL, InP QDs in nonane were coated on ZrO_2 layer by spin coating. Then organic hole transport layer (HTL), MoO_3 hole injection layer (HIL) and Al top electrode were sequentially deposited by the thermal evaporation. Figure 1c is the TEM cross section image of the interface between ZrO_2 ETL and InP QDs light emitting layer. Because the thicknesses of ZrO_2 and QD layers are about 8.9 and 5.9 nm respectively, we can estimate that the numbers of layers are three layers for ZrO_2 and one layer for InP QDs. Figure 1d displays the photoluminescence (PL) and EL intensities versus wavelength of our InP QDs. The peak wavelengths of PL and EL data are 586 and 600 nm respectively. The peak wavelength shift of 14 nm from same QD semiconductor is caused by the energy transfer from QDs with higher energy band gap to those with lower band gap in the closely packed QD layer and the electric-field induced Stark effect with tilted energy bands at increased driving voltage.[27–29] And we can observe that the FWHM value is 74 nm for PL and EL measurement respectively.

2.2. Hole Transport Layers for the Balance of Charge Injection

In the case of the light emitting devices which use the current driving scheme, the location of electron–hole recombination is very important. To improve the balance of charges injected from cathode and anode, we compared 4,4′-*N*,*N*-dicarbazole-biphenyl (CBP) and 4,4′-cyclohexylidenebis[*N*,*N*-bis(4-methylphenyl)benzenamine] (TAPC) which have been known as conventional HTL materials. Until now, in the case of Cd-based inverted QD-LED devices, CBP has been commonly used as HTL.[4,16,26,30] But, because the conduction band minimum and the valence band maximum of InP QDs are higher than those of CdSe QDs, there are large hole injection barrier and small electron blocking barrier between InP QDs and CBP layers (**Figure 2**a).[4] In **Figure 3**a, there is an additional emission peak at about 400 nm for the device with CBP HTL due to the electron–hole recombination in CBP layer caused by the unbalance of charge injection.[31] To eliminate this additional emission peak, we used another HTL material, TAPC, which shows small hole injection barrier between TAPC and MoO_3 and large electron blocking barrier between TAPC and InP QDs (Figure 2b). Therefore, when we used TAPC as HTL, we could eliminate the additional emission peak caused by electron–hole recombination in CBP layer (Figure 3a). Figure 3b shows the current density versus voltage characteristics for QD-LEDs with CBP and TAPC as HTL materials. In the QD-LEDs with TAPC, we can observe the ohmic conduction region ($J \propto V^1$) up to 4.5 V and the clear trap-limited-conduction region ($J \propto V^7$) from 4.5 to 10 V, followed by pseudo space-charge-limited conduction ($J \propto V^4$) at higher voltages.[5,17,26] Since the device shows only ohmic conduction behavior in the lower bias region, the current must flow directly between cathode and anode. If there is any barrier between two electrodes, the current will decrease. In the case of our devices, there are two carrier blocking barriers. One is the hole blocking barrier between QDs and ZrO_2 ETL and the other is the electron blocking barrier between QDs and HTL. Because the hole blocking barriers in two devices (with CBP and TAPC) are identical, we have only to consider the electron blocking barriers. If the electron blocking barrier is high, the direct current between two electrodes decreases. Therefore, since the device with TAPC have higher electron blocking layer, the current densities from TAPC-based QD-LED in the ohmic conduction region are lower than those of CBP-based device. We can also observe the higher current density of QD-LED with TAPC from 7 to 10 V because the hole injection barrier at TAPC/MoO_3 interface is smaller than that at CBP/MoO_3 interface and the carrier mobility of TAPC is higher than that of CBP ($\mu_{TAPC} = 1 \times 10^{-2}$ cm^2 V^{-1}s^{-1}, $\mu_{CBP} = 2 \times 10^{-3}$ cm^2 V^{-1}s^{-1}).[32,33] Based on the ohmic conduction behavior under 4.5 V, we can know that ZrO_2 ETL plays a role as a simple charge conductor

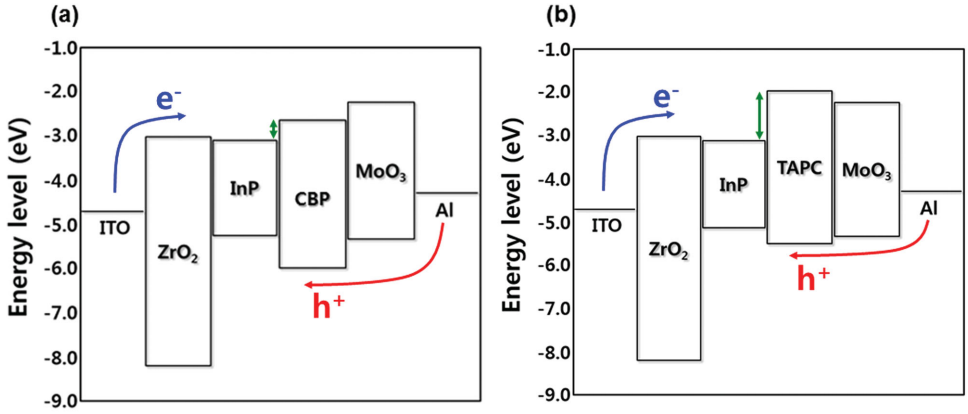

Figure 2. Energy band diagrams of InP QD-LEDs with a) CBP and b) TAPC as HTL. The hole injection barrier between TAPC and MoO_3 is smaller than that between CBP and MoO_3. And the electron blocking barrier between TAPC and InP QD is larger than that between CBP and InP QD.

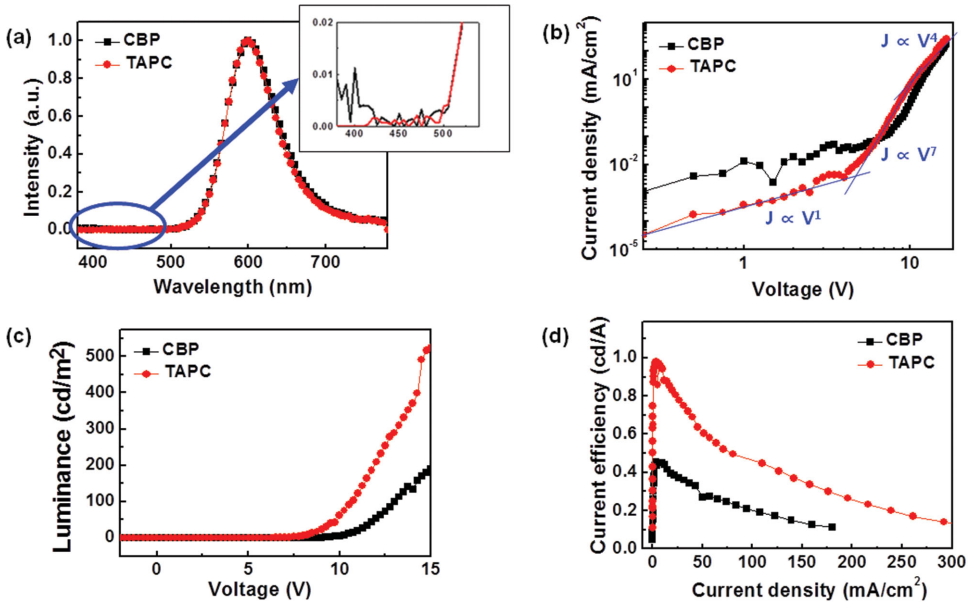

Figure 3. a) Electroluminescence spectra of InP QD-LEDs with CBP and TAPC HTLs and enlarged spectra between 380 and 540 nm (inset). There are additional emission peaks around 400 nm. b) Current density versus voltage characteristics of QD-LEDs with CBP and TAPC HTLs. In case of device with TAPC, there are the ohmic conduction region ($J \propto V^1$) up to 4.5 V and the clear trap-limited conduction region ($J \propto V^7$) from 4.5 to 10 V, followed by pseudo space-charge-limited conduction ($J \propto V^4$) at higher voltages. c) Luminescence versus voltage and d) current efficiency versus current density of QD-LEDs with CBP and TAPC HTLs.

which obeys Ohm's law sufficiently. And the trap-limited conduction behavior over 4.5 V means that there is light emission by electron–hole recombination in the QD layer as trap-center. Figure 3c,d show the maximum luminescence of 530 cd m^{-2} and the maximum efficiency of 1 cd/A for device with TAPC are twice as high as those of device with CBP due to charge balance in the QD layer. From these data, we can explain that TAPC increases the charge (hole) injection to QD layer and block the opposite charge (electron) efficiently. Therefore we chose TAPC as HTL materials for our InP QD-LEDs.

2.3. Process Optimization for ZrO_2 Electron Transport Layer

In the case of ZrO_2 nanoparticles, they have organic ligands, benzoic acid, on their surface for the passivation of ZrO_2 nanoparticles and the stable dispersion without agglomeration in solvent. But these surface ligands can disturb the charge flow in the electron transport layer into InP QD emission layer. To improve the charge injection and transport properties, we optimized process parameters to remove the surface ligands effectively. In Figure S2 in the Supporting Information, our InP QD-LED devices were fabricated with ZrO_2 ETLs annealed at 300 °C in various ambients such as air, vacuum, O_2 and N_2 by RTA. In Figure S2b in the Supporting Information, we can observe no additional emission peaks near 400 nm and same peak wavelengths at 600 nm for each case. The QD-LED device annealed in N_2 shows the brightest maximum luminescence (530 cd m^{-2}) and the highest current efficiency (≈1 cd/A) among four devices (Figure S2c,d, Supporting Information). This means that benzoic acid ligands can be removed by annealing in N_2 most effectively and we chose the N_2 for ZrO_2 annealing ambient.

In **Figure 4**, to find the optimized process temperature, we varied the annealing temperature from room temperature to 300 °C. Current density versus voltage data in Figure 4a also show the ohmic conduction region up to ≈4.5 V and the clear trap-limited conduction region after 4.5 V at all annealing temperatures. And, from Figures S2 in the Supporting Information, we can know that 300 °C annealing in N_2 ambient is the best annealing condition for our ZrO_2 ETL. But, since the differences of luminance and current efficiency data between 200 and 300 °C are too large, we tried to find the reasons for these large differences.

To analyze the annealing effect, the thermal gravimetric analysis (TGA) and the Fourier transform infrared spectroscopy (FTIR) analysis were performed. In **Figure 5**a, the ZrO_2 nanoparticles without annealing process show larger mass decrease of 6.7% up to 300 °C than that of ZrO_2 nanoparticles after 300 °C annealing process. This mass reduction means that residual water and solvent were removed and the organic ligands (benzoic acid) on the surface of ZrO_2 nanoparticles were evaporated because the boiling point of benzoic acid is around 249.2 °C.[34] But, in the case of annealed ZrO_2 nanoparticles, there is no mass reduction up to 300 °C because most of water, solvent and surface ligands on the ZrO_2 nanoparticles were removed during the 300 °C annealing process. Although we can observe the continuous mass decrease between 300 and 528 °C in both samples, it came from the removal of surface hydroxyl group strongly attached on the ZrO_2 nanoparticles. In Figure 5b, we analyze ZrO_2 nanoparticles by FTIR to check the existence of surface ligands after annealing process. The benzoic acid molecules have an O—H group and a C=O group and they show absorptions at around 3000 cm^{-1} for O—H group and around 1750 cm^{-1} for C=O group, respectively. Figure 5b shows the

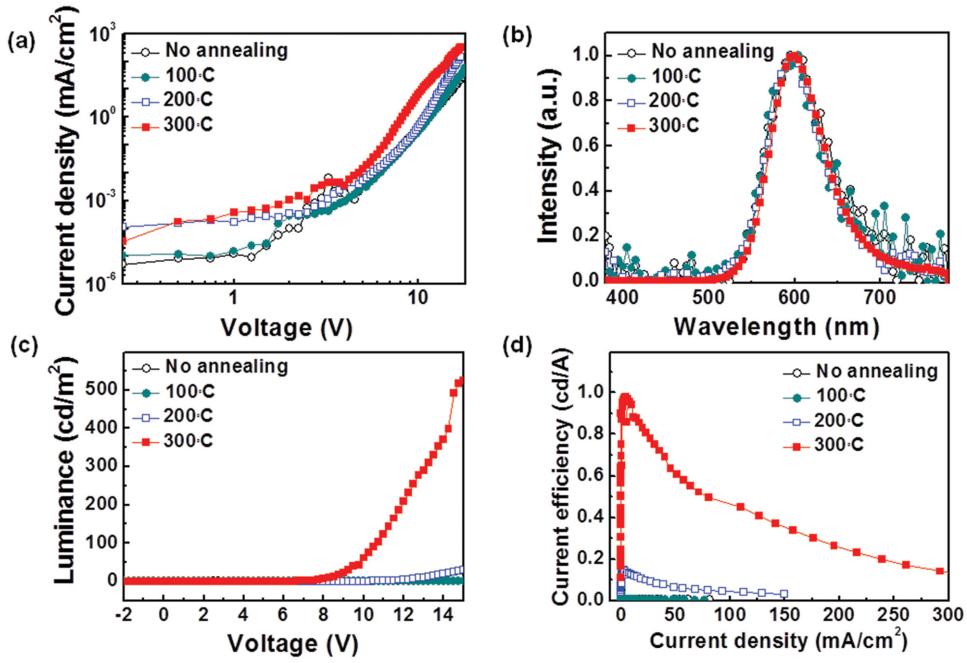

Figure 4. a) Current density versus voltage characteristics, b) electroluminescence spectra, c) luminescence versus voltage, and d) current efficiency versus current density of QD-LEDs with TAPC HTL and ZrO_2 ETL with various annealing temperatures from room temperature to 300 °C.

decrease of absorption for O—H and C O groups after 300 °C annealing in N_2 ambient and we can know that the benzoic acid molecules on the ZrO_2 nanoparticles were removed by annealing process.

2.4. Transparent QD-LEDs

To realize the transparent QD-LED device, we fabricated the transparent top electrode (IZO) on organic HTL by two-step sputtering process with thin oxide hole injection layer.[22] **Figure 6**a shows the device structure of our InP QD-LED with ZrO_2 HTL and transparent top electrode. To protect the organic HTL from sputtering damage, we increased the thickness of MoO_3 from 10 to 30 nm and used two-step sputtering process for IZO top electrode. This sputtering method used low-power (50 W) sputtering process to protect underlying organic layer and then high-power (150 W) sputtering process to maintain high conductivity (Table S1, Supporting Information). Figure 6b shows TEM cross section image of our transparent QD-LEDs, but it is not easy to distinguish IZO layers between with 50 and 150 W due to the same materials and composition. And we can also know that the TAPC HTL was not damaged by IZO two-step sputtering process. Figure 6c shows the transmittance data of several parts in our transparent QD-LED devices. IZO/MoO_3 layers and IZO/MoO_3/TAPC layers show the transmittance of more than 78% at 550 nm. We also measured the transmittance of whole device panel and it showed the transmittance of more than 74% and this value is similar to or higher than those of the conventional OLED using thin metal layers and the Cd-based QD-LED devices using graphene or silver nanowire as transparent top electrodes.[21,35,36]

Figure 7a shows the current density versus voltage of the devices with different top electrodes. In the case of Al electrode,

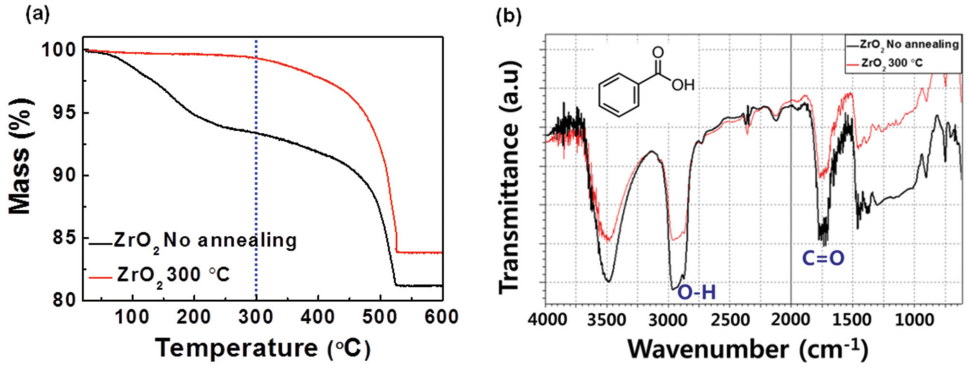

Figure 5. a) TGA and b) FTIR analysis of ZrO_2 nanoparticles before and after RTA in N_2 ambient at 300 °C. The benzoic acid molecules (inset) have an O—H group and a C═O group and they show absorptions at around 3000 cm^{-1} for O—H group and around 1750 cm^{-1} for C═O group, respectively.

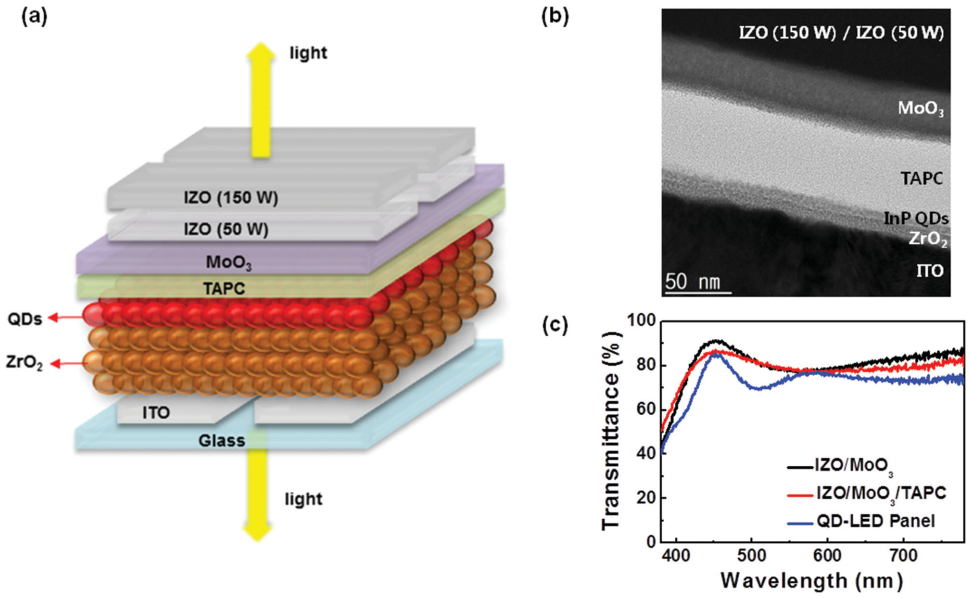

Figure 6. a) 3D schematic view of our InP QD-LED with ZrO_2 HTL and transparent top electrode. To protect the organic HTL from sputtering damage, we increased the thickness of MoO_3 from 10 to 30 nm and used two-step sputtering process for IZO top electrode. b) TEM cross section image of transparent QD-LED. It is not easy to distinguish IZO layers between with 50 and 150 W due to the same materials and composition. c) Transmittance data of several parts (IZO/MoO_3, IZO/MoO_3/TAPC, and whole device) in our transparent QD-LED devices. Transmittance of whole device is more than 74% at 550 nm.

it shows the best *J*–*V* characteristics among three devices. But, in the case of the device with IZO sputtered by using only 150 W, it shows very conductive properties at low operation voltages and there is no trap-limited conduction region. In the case of two-step sputtering process for IZO, although it shows slightly larger current density under 4 V than that of the device with Al, we can observe the trap-limited conduction region over 8 V which is related to the light emission from QDs. Figure 7b and c show the luminance and current efficiency characteristics of our transparent QD-LED. Because the transparent device emits the light to both top and bottom directions simultaneously, it shows lower performances than the device with Al top electrode. In Figure 3a, we can observe an additional peak at about 400 nm for the device with CBP HTL due to the e–h recombination in CBP layer caused by the unbalance of charge injection. When we used TAPC as HTL (Figure 2b), we could eliminate the additional peak. But this elimination of additional peak could be possible not due to charge-injection balance but

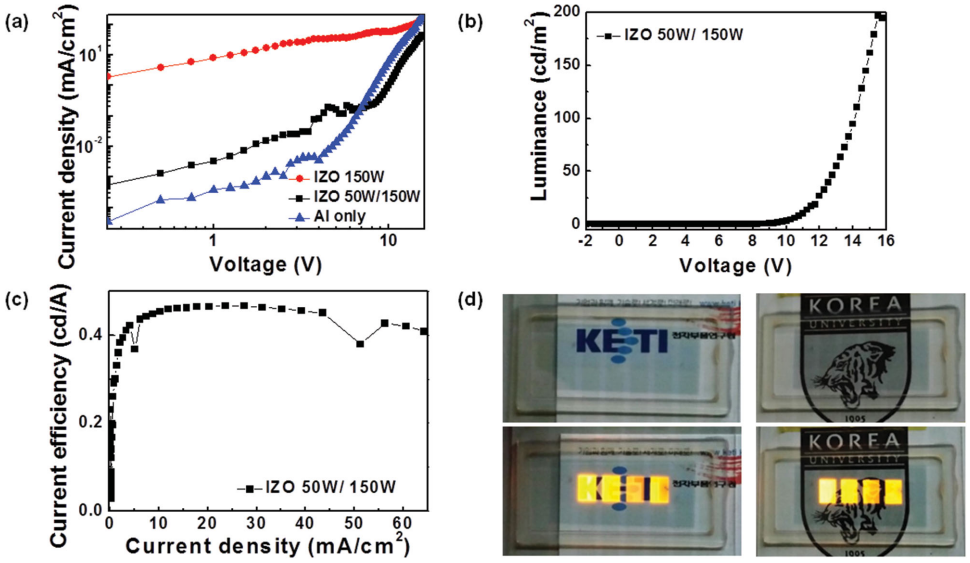

Figure 7. a) Current density versus voltage characteristics of the devices with different top electrodes. b) Luminance and c) current efficiency characteristics of our transparent QD-LED. Because the transparent device emits the light to both top and bottom directions simultaneously, the it shows lower performances than the device with Al top electrode. d) Photographs of our transparent device. When the device is off, we can see the background images very clearly through the transparent QD-LEDs. But, when the device is on, we can see the bright light-emitting pixels on the background images.

due to the larger electron blocking barrier between TAPC and InP QDs. There might be still charge-injection unbalance. In Figure 3d, the device shows roll-off at high current density because the balance of charges injected from anode and cathode is not kept. Therefore, the main cause of efficiency roll-off at high current must be Auger recombination due to the significant charging of quantum dots with excess electrons.[37] But we cannot observe the roll-off in Figure 7c. For the transparent QD-LED devices, we used transparent oxide electrode (IZO) and increased the thickness of MoO_3 (10–30 nm) to prevent the damage from sputtering process of IZO. In Figure 2 b, the hole injection barrier (HIB) between Al and MoO_3 is 1.1 eV and this barrier cannot be ignored. Although the HIL became thicker than before, the hole injection barrier between IZO and MoO_3 is 0.7 eV (Figure S3, Supporting Information). Because the HIB between anode and HIL decreased by 0.4 eV, the hole injection from anode could be enhanced and we could reduce the charging of QDs by excess electrons. Therefore, a roll-off of current efficiency was not observed in Figure 7c.

Finally, by using these technologies, we could realize fully transparent QD-LEDs with eco-friendly InP QDs and inorganic ZrO_2 HTL. Figure 7d shows the real photographs of our transparent device. When the device is off, we can see the background images very clearly through the transparent QD-LEDs. But, when the device is on, we can see the bright light-emitting pixels on the background images.

3. Conclusion

In conclusion, we have fabricated the transparent and eco-friendly QD-LED devices with Cd-free InP QDs as light emitting layer and inorganic ZrO_2 nanoparticles as electron transport layer by the optimization of post-annealing and the two-step sputtering process. The luminance and current efficiency of our QD-LED with Al top electrode are 530 cd m^{-2} and 1 cd/A respectively. When we used the two-step sputtering deposition process for the transparent electrode on organic semiconductors, we could realize the fully transparent QD-LED devices (T_{panel} > 74% @ 550 nm) with 200 cd m^{-2} and 0.47 cd/A successfully. We thus conclude that our transparent QD-LED could be a promising device to meet with the advent of next-generation transparent display era.

4. Experimental Section

The InP/ZnSe/ZnS multishell QDs were synthesized by heating-up method which is simple compared to conventional hot-injection method by removing manual injection process. A mixture of indium acetate and zinc octanoate was heated until a homogeneous solution was obtained, then dodecanethiol and tris(trimethylsilyl) phosphine were added in the mixture subsequently and heated to 300 °C for 45 min. In order to grow ZnSe shell, trioctylphosphine selenide was added first in the prepared InP core nanoparticles and heated to 280 °C for 10 min. Then, InP/ZnSe nanoparticles were capped with ZnS outer shell by adding trioctylphosphine sulfide followed by the heating to 280 °C for 10 min. The raw solutions of multishell QDs were purified several times by acetone induced precipitation and centrifugation, and the QD powders were redispersed in nonane for the device fabrication.[24,25]

The inverted organic/inorganic hybrid QD-LED devices were fabricated by following methods. 50 × 50 mm^2 ITO coated glass substrates were patterned by the conventional photolithography method and a wet etching process. Patterned ITO glass substrates were cleaned by acetone, methanol, isopropyl alcohol (IPA) and rinsed with deionized water and blown with N_2 and followed by ultraviolet ozone (UV/O_3) treatment for 5 min. For the ETL, ZrO_2 nanoparticles (PlasmaChem GmbH, average particle size : ≈3 nm) stabilized by benzoic acid were dispersed in a mixed solvent of methyl ethyl ketone (MEK) and Toluene. Then ZrO_2 nanoparticles solution was spin coated at 2000 rpm on the patterned ITO glass followed by RTA at various temperatures (from room temperature to 300 °C) and ambients (air, vacuum, O_2, and N_2). After the post-annealing of ETL, InP/ZnSe/ZnS core/multishell quantum dots in nonane solvent of 5 mg mL^{-1} were spin coated on the ZrO_2 ETL in a N_2 glove box. 4,4′-*N*,*N*′-dicarbazole-biphenyl (CBP, 60 nm) or 4,4′-cyclohexylidenebis[*N*,*N*-bis(4-methylphenyl)benzenamine] (TAPC, 60 nm) as HTL and MoO_3 (99.95%, 10 nm) layer as HIL were deposited by thermal evaporation. And aluminum (Al, 150 nm) anode was deposited with metal shadow mask by thermal evaporation. In the case of transparent QD-LED, thicker MoO_3 (30 nm) HIL by thermal evaporation and double-layered IZO(25 and 130 nm) sputtered by sequential radio frequency (RF) magnetron sputtering with two different power of 50 and 150 W were deposited. The fabricated devices were encapsulated by the encapsulation glass using UV sealant in the glove box with nitrogen.

To measure the optical characteristics of InP QD material itself, PL of diluted QD solution (0.5 mg mL^{-1}) was measured by Fluoro-Q2100 (K-MAC). A spectroradiometer (Minolta CS1000) was used for measurement of the EL spectrum and *J*–*V*–*L* (current density–voltage–luminance) was measured with an experimental setup consisting of a Keithley 2400 source meter and calibrated with a high-speed silicon photodiode (FDS 100) at ambient condition. The luminance and current efficiency were calculated from the photocurrent of photodiode and calibrated precisely with the luminance detected from the spectroradiometer. To measure the change of mass and chemical bonding for ZrO_2 nanoparticles with surface ligands before and after RTA treatment, TGA/DTA (DTG-60H, SHIMADZU) and FTIR (IRAffinity-1S, SHIMADZU) were used. The transmittance of the transparent QD-LED was measured by UV–vis Spectrophotometer (V-560, JASCO). The cross section images of devices and the thickness of ZrO_2 and QD layers were measured by focused ion-beam (Quanta 3D FEG, FEI) and transmission electron microscopy (JEM-2100F, JEOL).

Supporting Information

Supporting Information is available from the Wiley Online Library or from the author.

Acknowledgements

H.Y.K. and Y.J.P. contributed equally to this work. This work was supported by the Industrial Strategic Technology Development Program (10045145, Development of high performance (>70 cm^2 $V^{-1}s^{-1}$) chalcogenide TFT backplane and cadmium-free highly efficient (>30 cd/A) hybrid EL material/devices) funded by the Ministry of Trade, Industry and Energy (MOTIE, Korea).

Received: December 24, 2015
Revised: March 1, 2016
Published online: April 6, 2016

[1] S. Coe, W-K. Woo, M. Bawendi, V. Bulovic, *Nature*, **2002**, *420*, 800.
[2] Q. Sun, Y. A. Wang, L. S. Li, D. Wang, T. Zhu, J. Xu, C. Yang, Y. Li, *Nat. Photon.* **2007**, *1*, 717.

[3] L. Qian, Y. Zheng, J. Xue, P. H. Holloway, *Nat. Photon.* **2011**, *5*, 543.
[4] J. Kwak, W. K. Bae, D. Lee, I. Park, J. Lim, M. Park, H. Cho, H. Woo, D. Y. Yoon, K. Char, S. Lee, C. Lee, *Nano Lett.* **2012**, *12*, 2362.
[5] T-H. Kim, K-S. Cho, E. K. Lee, S. J. Lee, J. Chae, J. W. Kim, D. H. Kim, J-Y. Kwon, G. Amaratunga, S. Y. Lee, B. L. Choi, Y. Kuk, J. M. Kim, K. Kim, *Nat. Photon.* **2011**, *5*, 176.
[6] M. K. Choi, J. Yang, K. Kang, D. C. Kim, C. Choi, C. Park, S. J. Kim, S. I. Chae, T-H. Kim, J. H. Kim, T. Hyeon, D-H. Kim, *Nat. Commun.* **2015**, *6*, 7149.
[7] E. Jang, S. Jun, H. Jang, J. Lim, B. Kim, Y. Kim, *Adv. Mater.* **2010**, *22*, 3076.
[8] K-H. Lee, C-Y. Han, H-D. Kang, H. Ko, C. Lee, J. Lee, N. Myoung, S-Y. Yim, H. Yang, *ACS Nano* **2015**, *9*, 10941.
[9] J-S. Park, H. Chae, H. K. Chung, S. I. Lee, *Semicond. Sci. Technol.* **2011**, *26*, 034001.
[10] J. Meyer, P. Görrn, F. Bertram, S. Hamwi, T. Winkler, H-H. Johannes, T. Weimann, P. Hinze, T. Riedl, W. Kowalsky, *Adv. Mater.* **2009**, *21*, 1845.
[11] RoHS Guide Compliance, http://www.rohsguide.com/, accessed: 10, 2015.
[12] J. Lim, M. Park, W. K. Bae, D. Lee, S. Lee, C. Lee, K. Char, *ACS Nano* **2013**, *7*, 9019.
[13] Y. Kim, T. Greco, C. Ippen, A. Wedel, M. S. Oh, C. J. Han, J. Kim, *Nanosci. Nanotechnol. Lett.* **2013**, *5*, 1065.
[14] X. Yang, D. Zhao, K. S. Leck, S. T. Tan, Y. X. Tang, J. Zhao, H. V. Demir, X. W. Sun, *Adv. Mater.* **2012**, *24*, 4180.
[15] W-S. Song, S-H. Lee, H. Yang, *Opt. Mater. Express* **2013**, *3*, 1468.
[16] I. Jang, J. Kim, C. Ippen, T. Greco, M. S. Oh, J. Lee, W. K. Kim, A. Wedel, C. J. Han, S. K. Park, *Jpn. J. Appl. Phys.* **2015**, *54*, 02BC01.
[17] J. M. Caruge, J. E. Halpert, V. Wood, V. Bulovic, M. G. Bawendi, *Nat. Photon.* **2008**, *2*, 247.
[18] V. Wood, M. J. Panzer, J. E. Halpert, J.-M. Caruge, M. G. Bawendi, V. Bulovic, *ACS Nano* **2009**, *3*, 3581.
[19] N. Tokmoldin, N. Griffiths, D. D. C. Bradley, S. A. Haque, *Adv. Mater.* **2009**, *21*, 3475.
[20] C. J. Lee, R. B. Pode, D. G. Moon, J. I. Han, *Thin Solid Films* **2004**, *467*, 201.
[21] H-M. Kim, A. R. b. M. Yusoff, T-W. Kim, Y-G Seol, H-P. Kim, J. Jang, *J. Mater. Chem. C* **2014**, *2*, 2259.
[22] M. S. Oh, K. Lee, K. H. Lee, S. H. Cha, J. M. Choi, B. H. Lee, M. M. Sung, S. Im, *Adv. Funct. Mater.* **2009**, *19*, 726.
[23] F. C. Chen, Y. S. Lin, T. H. Chen, L. J. Kung, *Electrochem. Solid State Lett.* **2007**, *10*, H186.
[24] C. Ippen, T. Greco, A. Wedel, *J. Inf. Display* **2012**, *13*, 91.
[25] Y. Kim, C. Ippen, T. Greco, J. Lee, M. S. Oh, C. J. Han, A. Wedel, J. Kim, *Opt. Mater. Express* **2014**, *4*, 1436.
[26] J. Kim, Y. J. Park, Y. Kim, Y-H. Kim, C. J. Han, J. I. Han, M. S. Oh, *Electron. Mater. Lett.* **2013**, *9*, 779.
[27] V. Wood, M. J. Panzer, J-M. Caruge, J. E. Halpert, M. G. Bawendi, V. Bulovic, *Nano Lett.* **2010**, *10*, 24.
[28] B. S. Mashford, M. Stevenson, Z. Popovic, C. Hamilton, Z. Zhou, C. Breen, J. Steckel, V. Bulovic, M. Bawendi, S. C.-Sullivan, P. T. Kazlas, *Nat. Photon.* **2013**, *7*, 407.
[29] K-H. Lee, J-H. Lee, W-S. Song, H. Ko, C. Lee, J-H. Lee, H. Yang, *ACS Nano* **2013**, *7*, 7295.
[30] W. K. Bae, Y-S. Park, J. Lim, D. Lee, L. A. Padilha, H. McDaniel, I. Robel, C. Lee, J. M. Pietryga, V. I. Klimov, *Nat. Commun.* **2015**, *4*, 2661.
[31] V. Jankus, C. Winscom, A. P. Monkman, *J. Chem. Phys.* **2009**, *130*, 074501.
[32] J-W. Kang, S-H. Lee, H-D. Park, W-I. Jeong, K-M. Yoo, Y-S. Park, J-J. Kim, *Appl. Phys. Lett.* **2007**, *90*, 223508.
[33] P. Strohriegl, J. V. Grazulevicius, *Adv. Mater.* **2002**, *14*, 1439.
[34] W. M. Haynes, *CRC Handbook of Chemistry and Physics 91st ed*. Boca Raton, CRC Press Inc., Boca Raton, FL, USA **2010–2011**.
[35] J-T. Seo, J. Han, T. Lim, K-H. Lee, J. Hwang, H. Yang, S. Ju, *ACS Nano* **2014**, *8*, 12476.
[36] P. Jing, W. Ji, Q. Zeng, D. Li, S. Qu, J. Wang, D. Zhang, *Sci. Rep.* **2015**, *5*, 12499.
[37] W. K. Bae, Y-S. Park, J. Lim, D. Lee, L. A. Padilha, H. McDaniel, I. Robel, C. Lee, J. M. Pietryga, V. I. Klimov, *Nat. Commun.* **2013**, *4*, 2661.